MATHEMATICAL SIMULATION OF THE ELECTRICAL ACTIVITY OF THE HEART

Youssef Belhamadia[(1)], Yves Bourgault[(2)], and André Fortin[(3)]

(1) University of Alberta, Campus Saint-Jean.
(2) University of Ottawa, Department of Mathematics and Statistics.
(3) Université Laval, Département de mathématiques et de statistique.

I. INTRODUCTION

Heart diseases are the leading cause of death in the world. With the recent developments in scientific computing, numerical modeling starts to play a crucial role and provides the necessary tools for understanding rhythm disorders of the heart. However, efficient three-dimensional simulations of the electrical waves in the human heart are not yet feasible. The major difficulty is that the action potential is a wave with sharp depolarization and repolarization fronts.

The bidomain model is considered as the mathematical equations that give the best representation of the electrical waves in cardiac tissue (see Colli Franzone et al. [1]), and consists on the following equations:

$$\begin{cases} \dfrac{\partial V_m}{\partial t} - \nabla \cdot \left(G_i \nabla V_m\right) = \nabla \cdot \left(G_i \nabla \phi_e\right) + I_{ion}(V_m, W) \ \ on \ \ \Omega \\ \nabla \cdot \left((G_i + G_e)\nabla \phi_e\right) = -\nabla \cdot \left(G_i \nabla V_m\right) \qquad on \ \ \Omega \qquad (1) \\ \dfrac{\partial W}{\partial t} = g(V_m, W) \qquad on \ \ \Omega \end{cases}$$

Where $V_m = \phi_i - \phi_e$ is the transmembrane potential, ϕ_i and ϕ_e are the intracellular and the extracellular potentials, respectively, and W is the recovery variable. The functions $I_{ion}(V_m, W)$ and $g(V_m, W)$ represent the ionic model, and G_i and G_e are the symmetric intra- and extra-cellular conductivity tensors.

Modern cardiac ionic models results generally in a set of 10 to 60 ordinary differential equations. In this work, the simplified Aliev-Panfilov model (see Aliev and Panfilov [2]) is used to illustrate the adaptive method and consists of the following equations:

$$\begin{cases} I_{ion}(V_m, W) = kV_m(V_m - a)(1 - V_m) - V_m W \\ g(V_m, W) = \left(\varepsilon + \dfrac{\mu_1 W}{\mu_2 + V_m}\right)\left(-V_m - kV_m(V_m - a - 1)\right) \end{cases} \qquad (2)$$

The system of nonlinear partial differential equations coupled with an ordinary differential equation (1)-(2) is computationally very expensive, the major difficulties are due to the computational grids size that must be very fine to get a realistic three dimensional simulation of cardiac tissue. Many methods have been introduced in the literature to overcome these difficulties. Parallel computing techniques, for fixed spatial mesh, are used to reduce the computational time (see Colli Franzone and Pavarino [3]).

Recently, adaptive methods have been introduced in the context of electrocardiology, and consist in locating finer mesh near the depolarization and repolarization front position while a coarser mesh is employed away from the front (see Cherry et al. [4], Colli Franzone et al. [5]). In this work, a three-dimensional time-dependent adaptive method is used for the bidomain model. This method uses anisotropic mesh to reduce greatly the total number of element and therefore the computational time. A realistic geometry of the heart is used to show the performance and the accuracy of proposed algorithm. More details and discussion about this method is presented in Belhamadia [6,7] for the two-dimensional case and in Belhamadia et al. [8] for the three-dimensional with a monodomain model case.

This paper is organized as follows. Next section is devoted to the finite elements discretization while a brief description of the adaptive method is presented is section III. The last section presents three-dimensional numerical results showing the accuracy of the proposed method.

II. FINITE ELEMENT DISCRITIZATION

Several time-stepping strategies have been introduced for the bidomain model (see Bourgault et al. [9], and Keener and Bogar [10]). In all our numerical simulations, a fully implicit backward second order scheme (Gear) is employed as time discretization. The reader is refereed to [6] for more discussion about different time schemes and its impact on two-dimensional mesh adaptation. For instance, starting from V_m^{n-1} and W^{n-1} at time t^{n-1} and from V_m^{n} and W^{n} at time t^{n}, Gear scheme gives:

$$\begin{cases} \dfrac{\partial V_m}{\partial t}(t^{n+1}) \approx \dfrac{3V_m^{n+1} - 4V_m^n + V_m^{n-1}}{2\Delta t} \\ \dfrac{\partial W}{\partial t}(t^{n+1}) \approx \dfrac{3W^{n+1} - 4W^n + W^{n-1}}{2\Delta t} \end{cases}$$

A quadratic (P2) element is used for spatial discretization. The finite element variational formulation of the system (1)-(2) is straightforward. Newton's method is used to solve this nonlinear system at each time step. The obtained linear system is solved by iterative methods, the GMRES solver [11] with an incomplete LU decomposition (ILU) from the PETSc library [12].

III. TIME-DEPENDENT ADAPTIVE METHOD

Several authors estimate that a typical simulation of the whole heart may require about 10^7 mesh points, and therefore the memory requirements for structured mesh would rapidly exceed the capacity of available computers. In this paper, the computational mesh is refined near the front position, and the total number of mesh elements obtained is greatly reduced.

A brief description of the adaptive method for time dependent problems will now be presented. The error estimator is based on a definition of edge lengths using a solution dependent metric. The reader is refereed to Belhamadia et al. [8,13] for more details. Also, the bidomain model is a time-dependent problem and the mesh must be refined at each time step near the front position. Thus, a time-dependent algorithm is developed for this model and consists on the following:

1) Start from the solutions $V_m^{n-1}, V_m^n, W_m^{n-1}, W_m^n, \; and \; \phi_e^n$ and a mesh M^n at time t^n.

2) Solve the system (1)-(2) on mesh M^n to obtain a first approximation of the solutions $\tilde{V}_m^{n+1}, \tilde{W}_m^{n+1}, \; and \; \tilde{\phi}_e^{n+1}$ at time t^{n+1}.

3) Adapt the mesh by defining the metric through the composite variables $\dfrac{3\tilde{V}_m^{n+1} - 4V_m^n + V_m^{n-1}}{2\Delta t}, \dfrac{3\tilde{W}^{n+1} - 4W^n + W^{n-1}}{2\Delta t}, \tilde{\phi}_e^n, \; and \; \tilde{\phi}_e^{n+1}$

4) Reinterpolate $V_m^{n-1}, V_m^n, W_m^{n-1}, W_m^n, \; and \; \phi_e^n$ on mesh M^{n+1}

5) Solve the system (1)-(2) on mesh M^{n+1} for $V_m^{n+1}, W_m^{n+1}, \; and \; \phi_e^{n+1}$

The fully implicit backward second order scheme (Gear) used for time-stepping requires that the solutions at three time steps enter in the composite variables used in the adaptation algorithm. This is why step 3) is particularly important and the new mesh must properly capture the front position at time $t^{n-1}, t^n, \; and \; t^{n+1}$.

IV. THREE-DIMENTIONAL NUMERICAL RESULTS

A test problem will now be solved in three dimensions using a realistic heart geometry. This geometry has been obtained by dissection of a dog's heart, and the data is available from the Bioengineering Research Group at the University of Auckland (see Nash [14]). Homogeneous Neumann conditions are imposed on all boundaries. The initial transmembrane potential, the recovery variable, and the intra-cellular are given by:

$$V_m = \begin{cases} 1, & \sqrt{(x-15)^2 + (y-30)^2 + (z-50)^2} < 15, \\ 0, & \sqrt{(x-15)^2 + (y-30)^2 + (z-50)^2} \geq 15, \end{cases}$$

$$\phi_e = \begin{cases} -0.5, & \sqrt{(x-15)^2 + (y-30)^2 + (z-50)^2} < 15, \\ 0, & \sqrt{(x-15)^2 + (y-30)^2 + (z-50)^2} \geq 15, \end{cases}$$

$$and \quad W = 0.$$

This amounts to set non-zero potentials in a small region near the A.V. node. The symmetric conductivity tensors are $G_i = G_e = diag(1,1,1)$, and the other dimensionless parameters are given by:

$$\Delta t = 0.5 \qquad k = 8$$
$$\mu_1 = 0.2 \quad a = 0.15$$
$$\mu_2 = 0.3 \quad \varepsilon = 0.002$$

Figure 1 presents the transmembrane potential along a segment using two different uniformly refined meshes leading to 308127 dof and 1774439 dof. As could be seen, the transmenbrane potential position is very sensitive to insufficient mesh resolution.

Since a reference solution in three-dimension is very difficult to obtain, figure 2 presents a comparison between the solution obtained with regular mesh using 1774439 dof and with the adapted mesh using only 27400 dof. The two numerical solutions are almost the same. However, the number of elements is greatly reduced with the adaptive method since the

mesh is refined only in the vicinity of the front position while keeping sufficient resolution in other regions. The gain in computational time is very obvious since the total number of element is greatly reduced. The reader is refereed to [8] for quantitative results in the context of monodomain model.

Figure 3 shows a cross-section of the transmembrane potential at time $t = 60\ t.u.$ using regular and adapted mesh. This figure shows that the adaptive method clearly gives a smoother wave front. The adapted mesh is presented in figure 4 a), while a cross section of this mesh is presented in figure 4 b). This figure shows the use of the anisotropic mesh, which produces a concentration of the elements near the front location, leading to an accurate numerical solution.

V. CONCLUSION

In this work, an adaptive method for the bidomain model was presented. This method reduces the total number of elements and leads to an accurate three-dimensional numerical solutions. Realistic heart geometry has been used to illustrate the advantage of the proposed algorithm.

VI. REFERENCES

[1] P. Colli Franzone, L. F. Pavarino, and B. Taccardi. "Simulating Patterns of Excitation, Repolarization and Action Potential Duration with Cardiac Bidomain and Monodomain Models." Mathematical Biosciences, 197:35–66, 2005.

[2] R.R. Aliev and A.V. Panfilov. "A Simple Two-Variable Model of Cardiac Excitation."Chaos, Solitons and Fractals, 7(3):293–301, 1996.

[3] P. Colli Franzone and L. F. Pavarino. "A Parallel Solver for Reaction-Diffusion Systems in Computational Electrocardiology." Math. Model and Methods in Applied Sciences, 14(6):883–911, 2004.

[4] E.M. Cherry, H.S. Greenside, and C. S. Henriquez. "Effcient Simulation of Three-dimensional Anisotropic Cardiac Tissue Using an Adaptive Mesh Refinement Method". Chaos: An Interdisciplinary Journal of Nonlinear Science, 13(3):853{865, 2003.

[5] P. Colli Franzone, P. Deufhard, B. Erdmann, J. Lang, and L. F. Pavarino. "Adaptivity in Space and Time for Reaction-Diffusion Systems in Electrocardiology". SIAM Journal on Scientific Computing, 28(3):942{962, 2006.

[6] Y. Belhamadia. "A Time-Dependent Adaptive Remeshing for Electrical Waves of the Heart." IEEE Transactions on Biomedical Engineering, 55(2, Part-1):443–452, 2008.

[7] Y. Belhamadia. "An Efficient Computational Method for Simulation of the Two-dimensional Electrophysiological Waves." Conf Proc IEEE Eng Med Biol Soc. 2008; 2008: 5922-5.

[8] Belhamadia Y., Fortin A. and Bourgault Y. (2008), An Accurate Numerical Method for Monodomain Equations Using a Realistic Heart Geometry. Mathematical Biosciences. Submitted.

[9] M. Ethier and Y. Bourgault. "Semi-implicit time-discretization schemes for the bidomain model". SIAM Journal of Numerical Analysis, 46(5):2443{2468, 2008.

[10] J. P. Keener and K. Bogar. A numerical method for the solution of the bidomain equations in cardiac tissue. Chaos, 8:234-241, 1998.

[11] Y. Saad. "Iterative Methods for Sparse Linear Systems." PWS Publishing Company, 1996.

[12] S. Balay, K. Buschelman, V. Eijkhout, W. Gropp, D. Kaushik, M. Knepley, L. C. McInnes, B. Smith, and H. Zhang. PETSc "Users Manual. Technical Report ANL-95/11-Revision 2.1.6", Argonne National Laboratory, Argonne, Illinois, 2003. http://www.mcs.anl.gov/petsc/.

[13] Y. Belhamadia, A. Fortin, and É. Chamberland. Three-Dimensional Anisotropic Mesh Adaptation for Phase Change Problems. Journal of Computational Physics, 201(2):753-770, 2004.

[14] M. Nash. "Mechanics and Material Properties of the Heart using an Anatomically Accurate Mathematical Model." PhD thesis, University of Auckland, New Zealand, 1998.

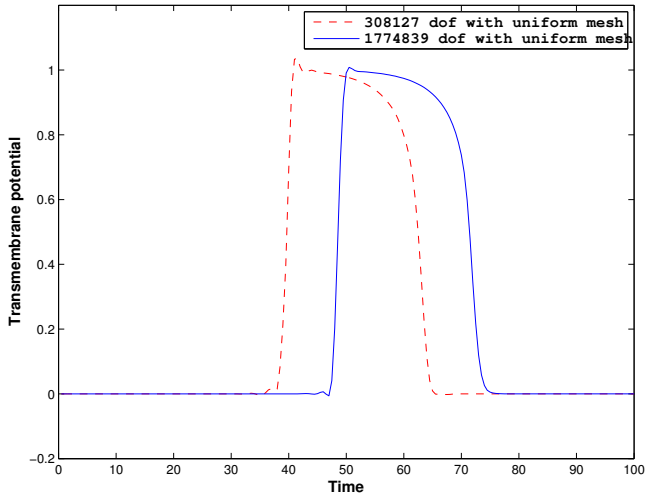

Figure 1: Transmembrane potential with two regular meshes

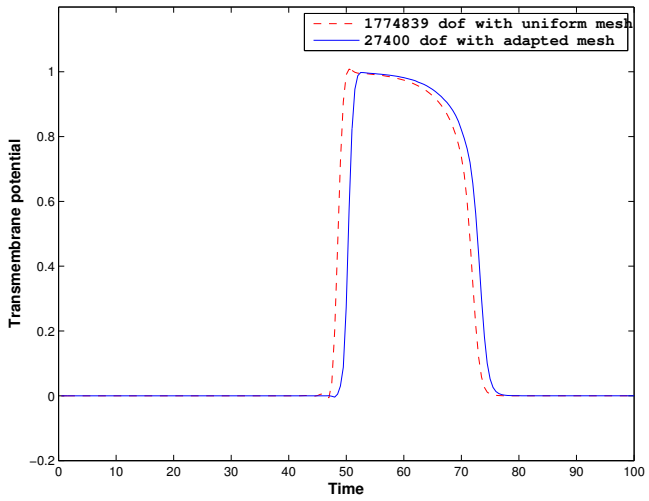

Figure 2: Transmembrane potential with regular and adapted mesh.

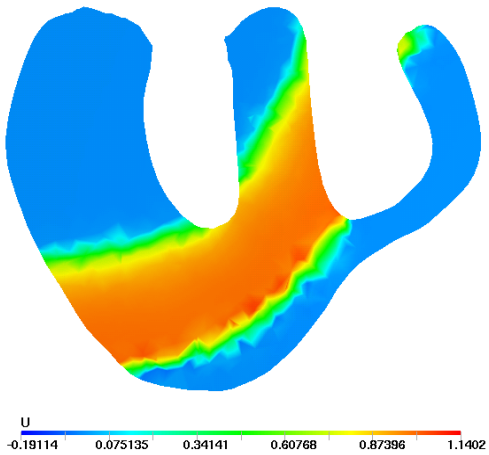

a) Uniform mesh: 308127 dof.

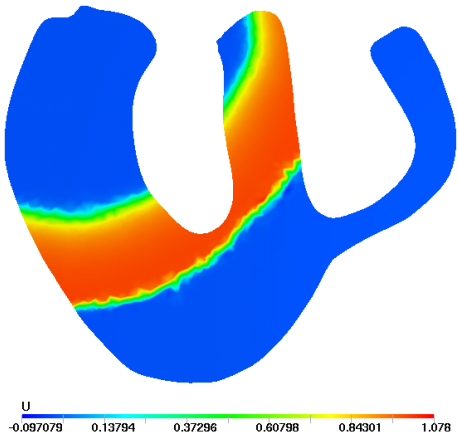

b) Uniform mesh: 1774439 dof.

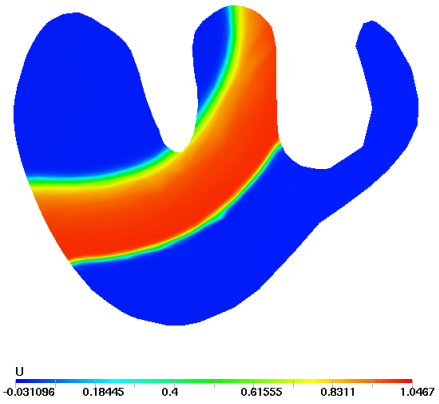

c) Adapted mesh: 27400 dof.

Figure3: Cross-section at $Z = 50$ of the transmembrane potential at time $t = 60\ t.u.$

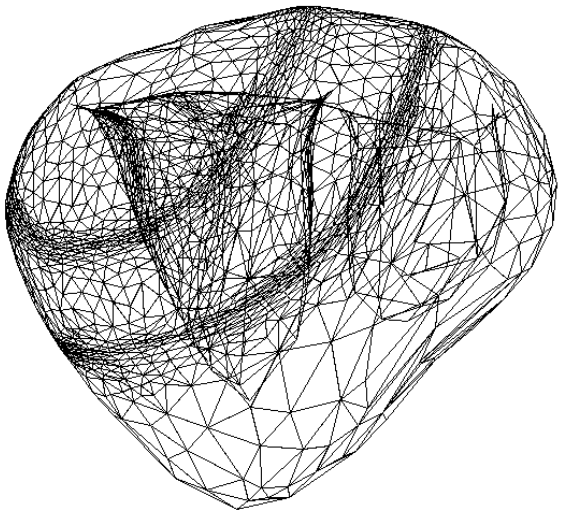

a) Mesh envelope

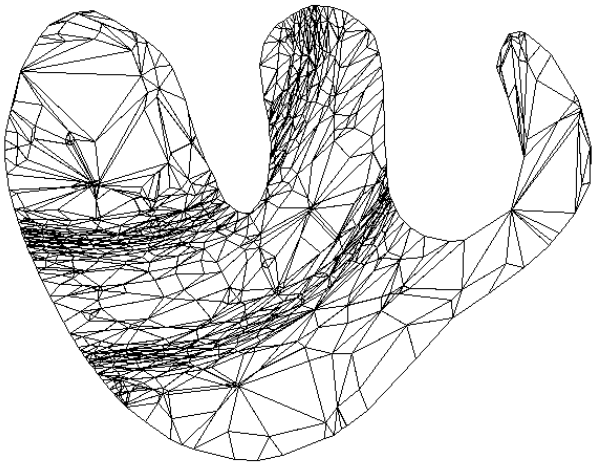

b) Cross-section at $Z = 50.$

Figure4: Adapted mesh at time $t = 60\ t.u.$